

Article

# Rotating Detonation Combustion for Advanced Liquid Propellant Space Engines

Stephen D. Heister <sup>\*,†</sup>, John Smallwood, Alexis Harroun , Kevin Dille, Ariana Martinez and Nathan Ballintyn 

School of Aeronautics and Astronautics, Purdue University, West Lafayette, IN 47906, USA

\* Correspondence: heister@purdue.edu

† Contribution for Liquid Rocket Engine edition of *Aerospace Propulsion*.

**Abstract:** Rotating (also termed continuous spin) detonation technology is gaining interest in the global research and development community due to the potential for increased performance. Potential performance benefits, thrust chamber design, and thrust chamber cooling loads are analyzed for propellant applications using liquid oxygen or high-concentration hydrogen peroxide oxidizers with kerosene, hydrogen, and methane fuels. Performance results based on a lumped parameter treatment show that theoretical specific impulse gains of 3–14% are achievable with the highest benefit coming from hydrogen-fueled systems. Assessment of thrust chamber designs for notional space missions shows that both thrust chamber length and diameter benefits are achievable given the tiny annular chamber volume associated with the rotating detonation combustion. While the passing detonation front drastically increases local heat fluxes, global energy balances can be achieved if operating pressures are limited to be comparable to existing or prior space engines.

**Keywords:** space propulsion; rotating detonation; continuous detonation



**Citation:** Heister, S.D.; Smallwood, J.; Harroun, A.; Dille, K.; Martinez, A.; Ballintyn, N. Rotating Detonation Combustion for Advanced Liquid Propellant Space Engines. *Aerospace* **2022**, *9*, 581. <https://doi.org/10.3390/aerospace9100581>

Academic Editor: Justin Hardi

Received: 25 August 2022

Accepted: 1 October 2022

Published: 7 October 2022

**Publisher's Note:** MDPI stays neutral with regard to jurisdictional claims in published maps and institutional affiliations.



**Copyright:** © 2022 by the authors. Licensee MDPI, Basel, Switzerland. This article is an open access article distributed under the terms and conditions of the Creative Commons Attribution (CC BY) license (<https://creativecommons.org/licenses/by/4.0/>).

## 1. Introduction

The concept of detonative propulsion was first conceived of by Zeldovich in a paper published in 1940, where he demonstrated theoretical efficiency gains from combusting propellants in a detonative mode vs. a deflagrative mode [1]. A variety of engine topologies have been suggested over the years, including pulse detonation engines and wave rotors, but the rotating detonation rocket engine (RDRE) approach has gained the most interest due mainly to its simplicity as compared to competing approaches that would demand highspeed valving to process reactants for a given detonative event.

Early works [2,3] in the latter part of the last century effectively proved that a stable rotating detonation could be attained but results were difficult to attain given the instrumentation capabilities at the time. Much of the progress in the modern era has been achieved in the present century given the availability of lower-cost, higher-capability, high-frequency instrumentation. A highly notable contribution in the RDRE realm came from the Bykovskii et al. study demonstrating high average combustion pressures in gas–gas (Propane–GOX), gas–liquid (Acetone–GOX), and liquid–liquid (Kerosene–LOX) propellant combinations [4]. A fairly recent review paper [5] describes gas/gas RDRE work as well as airbreathing studies using gaseous and liquid fuels. More recently, results have been obtained for liquid/liquid propellant injection using nitrogen tetroxide and monomethyl hydrazine storable propellants [6,7] as well as with hydrogen peroxide and a catalyst-loaded fuel based on the industrial solvent triglyme [8] as well as with gaseous oxygen and kerosene [9].

In 2021, two RDRE flight demonstrations took place. In collaboration with three Japanese Universities, the Japan Aerospace Exploration Agency (JAXA) successfully deployed a gaseous methane/gaseous oxygen RDRE from a sounding rocket and demonstrated ignition in space. The group was also able to measure a small torque believed to

be a consequence of viscous interactions of the detonation fronts with chamber walls [10]. In addition, Wolański et al. from the Lukasiewicz Institute of Aviation launched a small propane/nitrous oxide RDRE sounding rocket that reached an altitude of 450 m [11]. Hence, one might argue that the technology is maturing toward higher performance missions that will demand long duration and use of storable or cryogenic propellants.

Figure 1 highlights the general features of the RDE combustor as reactants are fed into an annular combustor chamber that may support one or more detonation waves. With proper operating conditions, the passage of the high-pressure detonation wave temporarily stops the flow of new reactants. This “aerovalving” feature permits the use of a conventional feed system such as those employed in current generation liquid rocket engine (LRE) combustors.

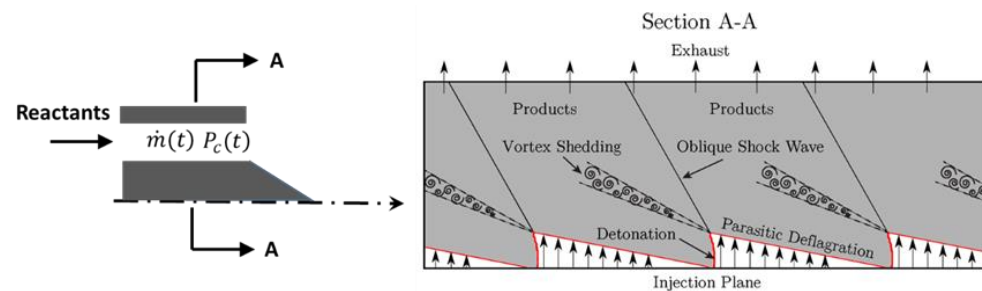


**Figure 1.** Topology of annular RDE combustor with time-dependent massflow and chamber pressure. Section A-A shows notional reactant fill region and shock/detonation wave structures with multiple waves present around the combustor annulus.

Subsequent recovery of the flows creates the triangular shaped “fill region” as noted in Figure 1. The boundary of this region places cold reactants in proximity to hot combustion products with potential for pre-ignition or “parasitic” deflagration prior to wave arrival.

The fear of parasitic deflagration reducing or eliminating detonations from the chamber has led researchers to shy away from traditional fuel-film cooling approaches employed in many existing LRE combustors. This reason, combined with very high heat transfer coefficients created by the passing detonation front, places chamber cooling as a major challenge for long-duration operation for realistic LRE missions demanding 10 s–100 s of seconds of continuous operation. While the RDRE combustion chamber volume is roughly an order of magnitude smaller than a conventional LRE combustor, the overall heat loads may be similar to or higher than the heat loads seen in today’s engines. Here, engine thrust level/size also enters as a consideration because in general, larger engines with higher propellant flows are easier to cool due to the relative scaling of wall area with thrust.

Limited design studies have been published to date based on space engine [12] and booster/launch engine [13] applications. The present work is aimed at improving on these results in making use of more recent chamber heating estimates that are coming from the community. The fact that space engines can utilize lower operating pressures than LREs that operate within the earth’s atmosphere is an important consideration given the RDRE cooling challenge. In addition, the annular combustor topology provides significant system length advantages that can be important for a number of space engine applications.

The proposed contribution will develop a preliminary design of one or more RDRE space engines for selected missions in order to address the advantages over existing or conventional deflagrative combustion approaches. Existing performance, nozzle design, and component weight models will be used to assess overall envelope and potential specific impulse, system length, and weight advantages relative to current or historical space engines. As chamber heating loads are a major element of the design, regenerative cooling jacket analyses will be conducted to enhance the fidelity of the analysis.

## 2. RDRE Performance

Fundamentally, performance benefits of RDREs are derived from reduced entropy production due to combustion at elevated pressure. This benefit presumes that the structure can be designed for the mean operating pressure and thus cannot respond to the short-lived high pressures behind the detonation front. Pre-compression reactants by a high Mach number shock front provides peak temperatures that substantially exceed those of constant pressure combustion devices operating at the same mean pressure. The detonation pressure ratio, DPR, lies at the center of these arguments. Assuming perfectly mixed reactants in a quasi-steady wave-based system, this parameter can be computed for various propellant combinations of interest for space propulsion. The NASA Chemical equilibrium analysis tool [14] is limited to use with gas/gas detonations but in the U.S., Livermore Laboratories has developed the Cheetah code [15] that can consider heterogeneous (gas/liquid) or condensed phase (liquid/liquid) systems. These codes are basically solving the classical Chapman/Jouguet (CJ) [16] detonation problem that presumes perfectly mixed reactants contained on all sides by a tube/chamber. Fundamentally, DPR depends strongly on the density of the fluids being detonated and is a fairly weak function of the overall average operating pressure in the system.

Figure 1 depicts a typical pressure waveform and DPR values for a variety of propellant combinations. The arrival of the detonation front occurs at the minimum pressure in the cycle,  $P_{\min}$ , while general design and operating conditions are typically prescribed at an average pressure. Average pressure is typically assessed using a capillary tube average (or attenuated) pressure, CTAP, measurement. This measurement is easily made by placing a pressure transducer at the end of a section of tubing that is connected at some location within the combustion chamber. High-frequency surface-mounted measurements have been difficult to obtain in RDREs due to the challenging thermal environments. Water-cooled or helium purged instrumentation has been shown to survive, but provides a substantial blemish on the tiny combustor wall.

The DPR values show impressive pressure rise under the perfectly mixed and perfectly contained assumption associated with rocket propellants as compared to an airbreathing system with lower overall energy addition per unit mass of reactant. In particular, the heterogeneous and condensed phase systems offer potential for huge combustion pressures as dense gas/liquid or liquid/liquid mixtures are converted to gases by the passing detonation front.

One of the most important classical results from the CJ detonation analysis is the wavespeed generated by the exothermic reactions downstream of the shock front:

$$v_{CJ} = \sqrt{2(\gamma_2^2 - 1)(c_{p1}T_1 + q)} \quad (1)$$

Here,  $v_{CJ}$  is wavespeed,  $c_{p1}T_1$  is specific heat and temperature of reactants,  $\gamma_2$  is the ratio of specific heats of the product mixture and  $q$  is the heat of combustion of the reactant mixture that tends to be the dominant parameter relative to  $c_{p1}T_1$ . Hence, to first order, the wavespeed is solely determined by the heat release in the region upstream of the choking point per the Chapman/Jouguet analysis. Actual RDREs with incomplete mixing and poor containment can still generate wavespeeds that approach or even exceed these theoretical limits, as the CJ analysis is based on a steady-state assumption (i.e., overdriven or “galloping” conditions can be generated by discrete injection sites). The high wavespeeds generated by detonation of rocket propellants is a challenging, yet enabling feature of the RDRE as combustion times drop into the 25–100  $\mu\text{s}$  range—literally an order of magnitude less than in conventional deflagrative burning rocket combustors. While these short timescales enable significantly shorter combustor lengths, mixture preparation on such timescales may require substantial injection pressure drops for RDRE applications—particularly for liquids that barely move under such timescales using established injector pressure drops for today’s engines.

Liquid/liquid system pressures would easily destroy any combustor should perfect containment be obtained as is assumed in the calculation. Successful implementation of these combinations will necessarily require preparation of the detonable mixture some distance from chamber walls. Here, the detonable mixture would be surrounded by chamber exhaust gases and the pressure would be greatly attenuated prior to hitting chamber walls. The liquid/liquid RDRE technology is in general very immature and open literature publications are limited to just a few groups [4,6–8]. The extent to which vaporization plays a role in cryogenic fluids such as liquid oxygen (LOX) or high vapor pressure propellants such as nitrogen tetroxide (NTO) has not been established to any significant degree. Our group has made some initial efforts using the Cheetah tool with various assumptions regarding mixedness with exhaust products [17,18]. In general, these models generate more questions than answers, primarily due to the computation of real gas conditions at the gigantic pressure levels predicted by the Cheetah code.

Thermodynamic behavior of the RDRE is often approximated with an Atkinson cycle involving shock compression and constant volume heat addition [19]. As with constant pressure combustion devices, the nozzle performance is ignored in these basic thermodynamic analyses that are necessarily upper bound estimates. The most comprehensive performance estimates to date have focused on gas/gas propellant systems. Even under the assumption of perfect mixing and reactant containment within the detonation channel, numerous loss mechanisms exist due to multidimensional effects and non-axial flow produced primarily near the detonation front. One of the most important departures is with regard to nozzle performance [20] since this component will see a whole range of pressures as different portions of the wavefront are exhausted. In this respect, the RDRE nozzle operating in the atmosphere is only “on design” at a single point in the pressure waveform shown schematically in Figure 1. In the vacuum of space, the chamber-to-ambient pressure ratio is always infinite and nozzle size tends to be set more by packaging constraints so there is a distinct advantage for applying the time-varying pressure waveform in space conditions.

A quasi-steady performance treatment was initially developed by Stechmann [21] and subsequently published with colleagues [22]. The model assumes an empirically based pressure waveform to compute quasi-steady conditions for assessing combustion and nozzle performance at various stages in the cycle. The tool uses an empirically based pressure history such as those shown in Figure 2 and performs an integration of conditions (massflow, thrust coefficient, characteristic velocity,  $c^*$ ) based on instantaneous pressure under a quasi-steady assumption. The model does not account for any heat losses, residual swirl, unmixedness and detailed multidimensional expansion of products from discrete injection sites. Hence results may be regarded as a reasonable upper bound on what may be attained. The annular topology of the RDRE combustion chamber naturally integrates into aerospike-type nozzle designs with a couple different topologies as noted in Figure 3. The flared configuration is preferred for high expansion area ratio applications such as those in a space engine. As the model assumes perfect mixing and neglects multidimensional and frictional effects, results must be regarded as upper bounds.

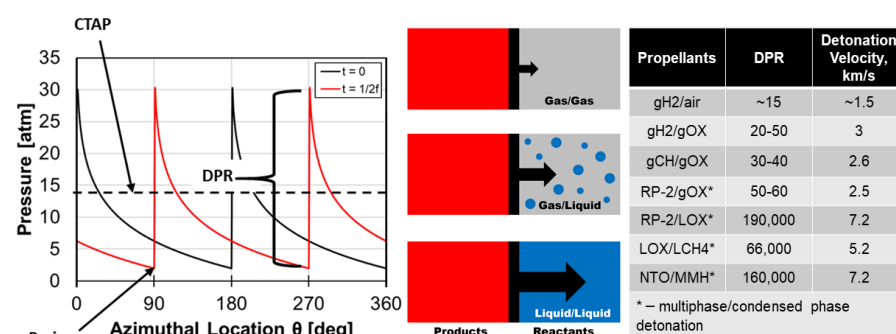


**Figure 2.** Detonation pressure ratios (DPR) and detonation velocity for numerous propellant combinations involving gaseous and liquid reactants.

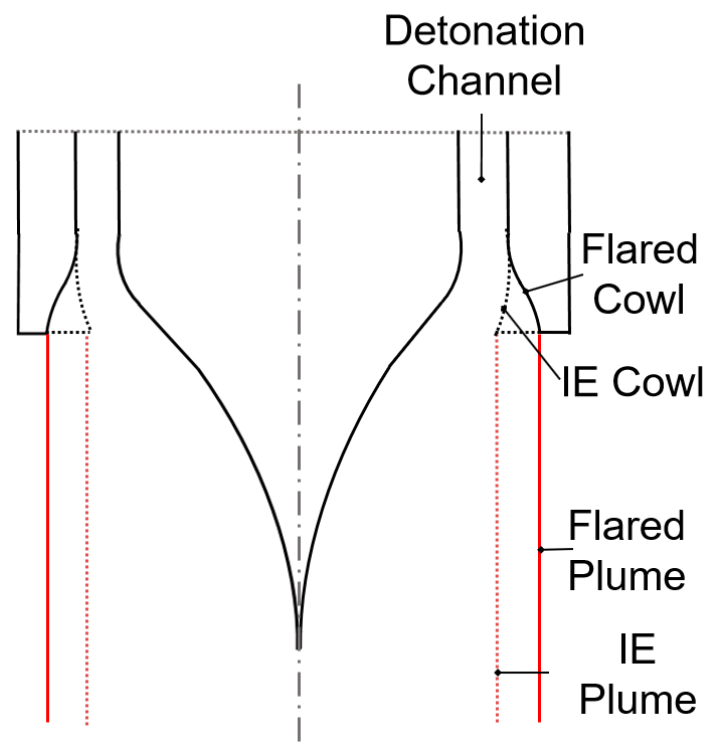


**Figure 3.** Internal expansion (IE) and Flared nozzle topologies that may be employed in RDRE. The flared configuration would be preferred for large expansion area ratio space engine applications and is the focus of the present study.

Propellant combinations assumed for the study include:

- Gaseous oxygen/kerosene (gOX/RP-2)—this combination applies to oxidizer-rich staged combustion engines currently under study for use in some space engine applications
- Liquid oxygen/gaseous methane (LOX/gCH<sub>4</sub>)—this combination is of interest for a number of launch providers and would result from vaporization of liquid methane in a cooling jacket for use in an expander or fuel-rich staged combustion engine
- Liquid oxygen/gaseous hydrogen (LOX/gH<sub>2</sub>)—this combination is employed in numerous space engines, primarily with an expander cycle that derives power from vaporized hydrogen that has extracted energy in the combustor regenerative cooling jacket
- Gaseous oxygen/gaseous hydrogen (gOX/gH<sub>2</sub>)—this propellant combination would result from use in a full-flow expander cycle engine where both cryogenic propellants are employed as coolants and turbine drive fluids
- Hydrogen peroxide/kerosene (HP/RP-2)—this is an alternative storable propellant combination that has received some attention over the years but has not been used in an operational space system to our knowledge. For the purposes of the study, the authors assume that the HP is 90% concentration and has been heated and vaporizes upon injection. While this may not be practical, it does provide some insight into general performance using heterogeneous detonation characteristics, i.e., it removes uncertainties associated with modeling fully condensed phase detonative performance

The optimal oxidizer/fuel mixture ratio (OF) was determined for each propellant combination to maximize vacuum specific impulse ( $I_{spv}$ ) for a notional CTAP of 10 atm and a nozzle expansion ratio of  $\epsilon = 100$ . Using this result, the specific impulse behavior of each of the six propellant combinations is summarized in Table 1. This table also includes assumed propellant temperatures in the optimization as well as a comparison against a constant pressure (CP) combustion engine with the same operating pressure and nozzle expansion ratio. The OF ratio was optimized for the CP engine in order to provide a useful comparison of potential performance enhancement. Table 1 also includes average characteristic velocities,

$C^*$ , as computed from CEA at the conditions noted for the CP engine, and as computed using the waveform-averaged technique from [22,23] for the RDRE.

**Table 1.** Optimal mixture ratios and performance comparison with constant pressure (CP) combustion engine for numerous RDRE propellant combinations, CTAP = 10 atm,  $\varepsilon = 100$ .

Propellants	Temp, K	RDRE Conditions			CP Engine Conditions			Perf. Gain, %
		OF	$C^*_{avg}$ , m/s	Ispv, s	OF	$C^*_{avg}$ , m/s	Ispv, s	
gOX/RP-2	400/400	2.3	1857	386	2.7	1765	375	3.0%
LOX/gCH4	90/300	2.8	1910	397	3.4	1812	384	3.5%
LOX/gH2	90/300	2.8	2680	538	4.2	2456	482	11.7%
gOX/gH2	200/300	2.6	2750	554	4.2	2472	486	14%
HP/RP-2	400/400	7.4	1654	347	8	1608	330	4.8%

For the conditions noted, potential performance gains range from 3 to 14%. These values would likely be regarded as upper bounds achievable given that the analysis does not account for frictional or shock losses attributed to the trailing oblique shock shown in Figure 1. Of course, other loss mechanisms also exist for the CP engine so the advantage shown still shows promise for the RDRE given the fidelity of the analysis. As with the prior studies [22,23] hydrogen-fueled systems offer the greatest advantages but tend to optimize at very low mixture ratios as indicated in Table 1. From a systems level perspective, this conclusion would need to be revisited given the size of the hydrogen tank implied from these results. In addition, the fast-kinetic response of hydrogen fuel has inhibited realization of the predicted performance gains. Using a transverse jet hydrogen injector, Stechmann [21] found that the hydrogen jets themselves tended to serve as flameholders when used in transverse jet injection scheme and as a result only deflagrative performance was realized. Alternate injector concepts may help alleviate this issue but this remains as a challenge to the community.

Given the large sensitivity of upper stage systems to even small improvements in specific impulse, the kerosene/RP-2 and methane-fueled options also offer promise. The slow kinetic response of methane fuel makes it an ideal RDRE fuel in many respects as parasitic deflagration prior to detonation wave arrival may be minimized. As a result, a number of groups around the world have demonstrated rotating detonations of this fuel (in gaseous form) with gaseous oxygen at substantial operating pressures. Work with liquid kerosene is more limited but successful detonations have been reported in oxygen [9] and air [24] at significant operating pressures. To the authors' knowledge, no results have yet been published on the HP/RP-2 system but the theoretical results do point to potential advantages there that would make up some of the deficit HP has with respect to LOX.

Systems with hydrogen/oxygen as propellants show performance benefits up to 14% higher than their constant pressure combustion counter-part, much higher than the 3–5% performance gains shown for the other propellants considered. Detonation-based combustion out-performs constant pressure combustion by releasing heat after being processed by the leading shock of the detonation wave. This shock increases the static pressure of the reactants, leading to entropy production rates lower than heat release at lower pressures. Additionally, the shock increases the static temperature of the reactants prior to any heat being released, leading to hotter post-combustion temperatures than what is possible via constant pressure combustion. Hydrogen/oxygen detonations show the largest performance benefit of the considered propellants because these detonations have a high degree of shock-heating without as large of a detonation pressure ratio when compared to the other propellants. The lower pressure ratio leads to less stagnation losses when averaging over the entire RDE blowdown cycle [22].

Results in Table 1 certainly offer a strong motivation for further study of the RDRE space engine application and numerous groups around the world are continuing to further

the technology. Unfortunately, the sensitive nature of performance measurements has precluded formal publication of recent work from many groups including our own. However, the Ref. [2] study does report mean chamber pressures that exceed theoretical limits of constant pressure combustion and that has served as motivation for many groups around the world to investigate the technology.

Using the five propellant combinations noted in Table 1 at the optimal OF determined for the RDRE based on the performance analysis tool, variations in performance with nozzle size for a chamber pressure of 10 atm are depicted in Figure 4. As with constant pressure combustion engines, vacuum performance is relatively insensitive to operating pressure (very little differences were present up to 40 atm operating pressure) and thus was neglected for this chart. Performance benefits become more modest at larger nozzle expansion ratios.

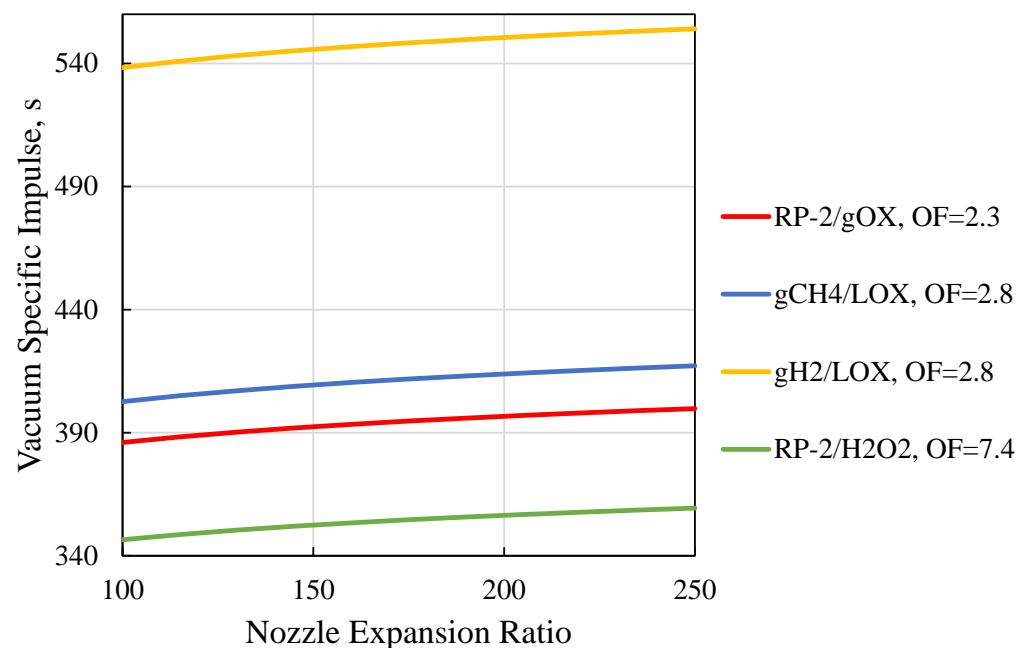


**Figure 4.** Theoretical RDRE performance variation with nozzle expansion ratio at 10 atm chamber pressure using the Stechmann et al. [22] performance model for the propellant combinations noted in Table 1.

### 3. RDRE Thrust Chamber Design

The thrust chamber topology assumed for this study is highlighted in the left schematic in Figure 5 with cold reactants (blue lines) entering at the top of the annulus and hot products (red lines) feeding the annular nozzle. This is perhaps the simplest possible thrust chamber topology with an annular chamber of mean radius  $R_c$  and length  $L$  with an annular gap  $\Delta$ . The airbreathing RDE community has studied “throated” combustors employing various chamber/throat area contraction ratios and many designs do not incorporate the flared nozzle cowling depicted in the sketch. The incorporation of an area contraction within the combustion chamber leads to reflected waves that can interact with the prime detonation front in deleterious manner. Prior work with gOX/gCH<sub>4</sub> propellants [21] revealed that incorporation of a throat entirely killed detonation behavior (presumably for this reason), but others have successfully demonstrated throated configurations. For the purposes of the study, this minor design difference would not necessarily affect conclusions.

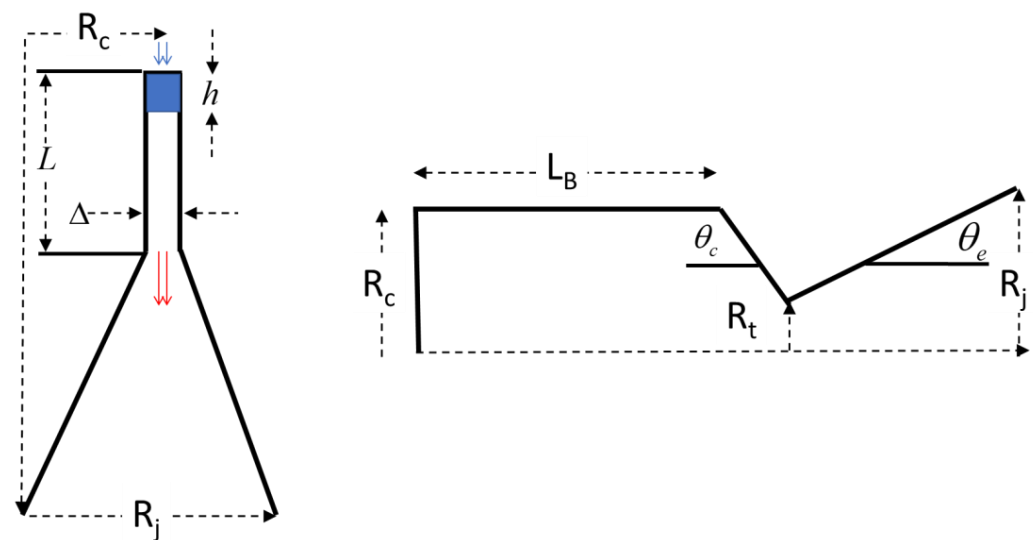


**Figure 5.** (l) RDRE thrust chamber design assumed for the study (r) Companion CP combustor geometry.

For the large expansion ratios demanded of a space engine, the outer nozzle cowling shown in Figure 5 will permit capture of pressure forces/thrust in the vacuum of space. The cooling jacket is assumed to extend to the terminus of the chamber centerbody with resulting exit radius,  $R_j$ . An uncooled nozzle extension could then be included to access the full expansion radius,  $R_e$ , set by the desired overall nozzle area ratio. To date, detailed design of the nozzle contour in the existing literature has employed techniques used in CP engines, i.e., a quasi-steady method of characteristics solution to determine the inviscid contour with potential adjustments for the local boundary layer momentum thickness. This level of detail will not be included in the present work.

In [4], authors provide criteria for chamber gap and length based on the detonation cell size. In practice, this quantity is submillimeter for highly detonable rocket propellants and hence these limiting criteria do not readily apply in this situation. In general, the chamber radius, thrust level and operating pressure are selected as the prime design variables. The chamber gap size is then determined from massflow considerations to deliver the necessary propellant flowrate at the desired operating pressure with the propellant combination of interest.

Perhaps the most difficult parameter to set is the overall chamber length,  $L$ . The blue region noted in Figure 5 is denoted the “fill height”,  $h$ . This represents the average or maximum penetration of reactants prior to wave arrival and consumption of the mixture. It can be viewed as the maximum axial extent of the fill region as shown in Figure 1. Predicting fill height a priori is very challenging as one would need to know both the wavespeed and the number of waves present around the annulus. Predictive capabilities for these parameters are becoming available in simple gas/gas combustors with high resolution large eddy simulation codes, but in general there is no good way to estimate  $h$  from simpler analytic models or for mixtures containing one or more liquids or supercritical fluids.

Fill heights/wave topologies are known to vary strongly with injector configurations and propellant injection conditions (i.e., temperature). Given the complexity, we will rely on historically successful combustor lengths of  $L = 1\text{--}3$  inches (2.5–7.5 cm) as being representative. In fact, these dimensions are likely longer than they need to be if many waves are present, but ignition of the combustor becomes less arduous the larger the  $L$  value so this will ultimately be a consideration especially for space engine vacuum ignition. Recently, Japanese researchers have successfully demonstrated vacuum ignition with a chamber 6 cm in length, but this chamber also had an area constriction of roughly 30% to form a throat [10].

#### 4. Comparing RDRE and CP Engine Thrust Chamber Design

The integration of the nozzle into the annular chamber geometry, combined with the small chamber volumes, has promise to reduce RDRE engine envelope when compared to a CP combustion engine. The total surface area to be cooled is of course a global consideration in thrust chamber assembly design. While the fast reaction times in the RDRE lead to chamber volumes roughly an order of magnitude smaller than CP combustors, that volume is wrapped in an annular geometry that tends to increase surface area over that of a cylinder. Prior studies for larger engines [12,13] revealed that the total surface area to be cooled for the RDRE was substantially less than that of a comparable CP engine, but this was for high thrust engines and a more general treatment is desired to assess behavior with thrust level. Assuming ideal quasi-steady flow, the throat area of the combustor is related to propellant massflow and average operating pressure,  $P_c$ :

$$A_t = \dot{m} C^*_{avg} / P_c \quad (2)$$

For the RDRE chamber, the throat/chamber area is dependent on both chamber radius and gap size, the ratio of which must remain small in order to provide similar distances for wave travel around the annulus. From various published results,  $0.075 < \Delta/R_c < 1$  [6,21]. This criterion, combined with Equation (2) permits computation of chamber dimensions as a function of massflow for a given average operating pressure for the RDRE chamber.

For the notional CP engine design, the length of the barrel section,  $L_B$ , can be determined from the chamber contraction area ratio,  $CR$ , and the chamber characteristic length,  $L^*$  [25]:

$$L_B = \frac{L^*}{CR} \quad (3)$$

Historical values for  $L^*$  vary from 0.5 to 1.0 m for systems using hydrogen fuel and 0.7 to 1.3 m for the other propellant combinations in Table 1 [25]. Low chamber pressure space engines have contraction area ratios in the range  $1.3 < CR < 10$  varying from very large to very small thrust level applications. For the conventional combustor, the radius at the terminus of the cooling jacket is computed:

$$R_j = \sqrt{\varepsilon_j A_t / \pi} \quad (4)$$

where  $\varepsilon_j$  is an input jacket expansion area ratio. The same dimension is applicable for the RDRE if the cooling jacket extends beyond the plug terminus. If this is not the case, the outer/inner radii to the annulus are:

$$R_j)_{outer/inner} = R_c \pm \frac{\varepsilon_j A_t}{4\pi R_c} \quad (5)$$

Note that this may not be the full engine expansion as cooling limits may make it desirable to utilize a radiation cooled Niobium skirt (or equivalent) to further enhance performance. Given these considerations, the computed geometry may differ from the case shown in Figure 5 where both RDRE nozzle surfaces terminate at the same axial location.

The analysis ignores wall surface area on the injector face. For a CP engine, heat fluxes here are mainly due to radiation, but in the RDRE there can be a highly convective environment although the surface area is quite small and injection orifices obviously reduce the total area to be cooled. To this extent, the RDRE wall areas reported may be viewed as a *lower* bound.

We spare the readers the tedium of the straightforward computation of wall area from surface areas of cylinders, frustums, and cones. Results from the study are reported in Figures 6 and 7 and Tables 2 and 3 respectively. Table 2 summarizes model inputs for empirical parameter and nozzle/chamber angles as mentioned above. The inputs for the CP engine were adjusted to reproduce the RL-10 geometry described in Ref. [25]. The  $L^*$  value for this engine is on the lower end of values reported [25] given the fast-

burning hydrogen fuel and was adjusted to match RL-10 chamber length accounting for the 45-degree conical chamber convergence angle assumed. In addition,  $\theta_e$  was adjusted to match the length of the contoured RL-10 nozzle.

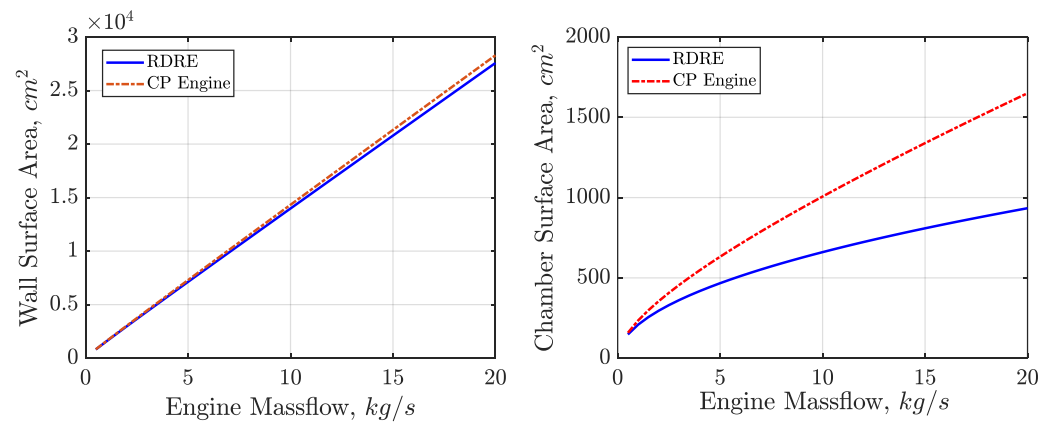


**Figure 6.** Surface area comparison. (l) total surface area. (r) chamber surface area.

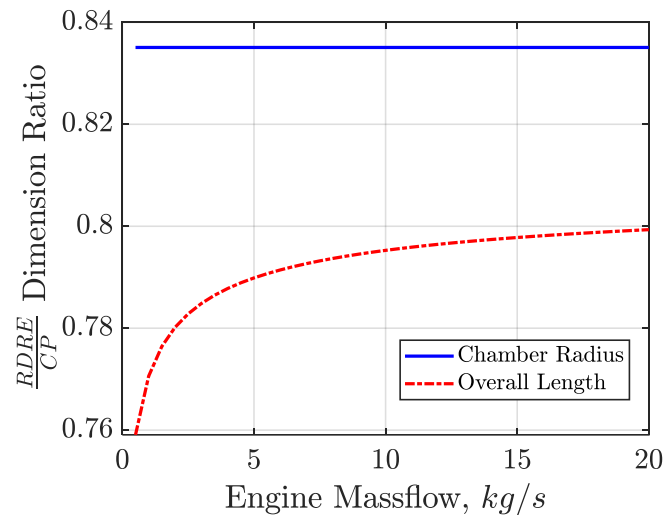


**Figure 7.** Comparison of envelope dimensions between RDRE and CP chambers.

**Table 2.** Summary of baseline inputs for wall surface area computation.

Parameter, Units	Value
$P_c$ , atm	33
$c^*$ , m/s	2385
L, cm	6
$\Delta/R_c$	0.15
$L^*$ , cm	45
CR	4.78
$\varepsilon_j$	61
$\theta_c$ , degrees	45
$\theta_e$ , degrees	19

**Table 3.** Sensitivity of chamber dimensions and surface area to design inputs at a massflow rate of 10 kg/s.

Parameter	$\frac{A_{c, RDRE}}{A_{c, CP}}$	$\frac{L_{tot, RDRE}}{L_{tot, CP}}$	$\frac{R_{c, RDRE}}{R_{c, CP}}$
$P_c$ , 25/33/41 atm	0.62/0.66/0.68	0.8/0.8/0.79	0.84/0.84/0.84
$c^*$ , 1700/2385 m/s	0.7/0.66	0.79/0.8	0.84/0.84
$\frac{\Delta}{R_c}$ , 0.1/0.15/0.2	0.8/0.66/0.57	0.75/0.8/0.72	1.0/0.84/0.82
$L$ , 3/6/9 cm	0.33/0.66/0.98	0.77/0.8/0.82	0.84/0.84/0.84
$L^*$ , 45/90 cm	0.66/0.4	0.8/0.73	0.84/0.84
$\frac{3}{4}$ 3/4.78/7	0.67/0.66/0.59	0.77/0.8/0.69	1.0/0.84/0.8
$\epsilon_i$ , 20/40/61	0.66/0.66/0.66	0.64/0.75/0.8	0.84/0.84/0.84

Figure 6 shows surface area comparisons for the inputs provided in Table 2. The total surface areas (left plot) are nearly equivalent as they are dominated by the larger nozzle contributions, but as can be seen in the right plot the RDRE chamber surface area is less than that of the CP chamber over the entire range of engine sizes considered with the disparity in areas increasing with thrust level/engine size. While the RDRE  $c^*$  value will be slightly higher per Table 1, the 2385 m/s value was used for both engines in this comparison. Interestingly, one can prove (for the simplified chamber/nozzle geometries employed) that the nozzle areas for both systems are identical, i.e., the inward and outward expansion surfaces of the RDRE add to precisely the same surface area as a conventional nozzle with the same throat area and expansion ratio, i.e., both designs reflect the diameter of a streamtube expanded to the same pressure with the same inlet conditions.

Working through the chamber surface area from the geometry in Figure 5 and assuming  $\Delta/R_c \ll 1$  one can show that the RDRE chamber surface area scales with the square root of the massflow:

$$A_{c-RDRE} = 4L \sqrt{\frac{\pi \dot{m} c^*}{P_c (\Delta/R_c)}} \tag{6}$$

whereas the CP chamber has both square root and linear dependence on massflow:

$$A_{c-CP} = 2L * \sqrt{\frac{\pi \dot{m} c^*}{P_c CR}} + \frac{\dot{m} c^* (CR - 1)}{P_c \sin \theta_c} \tag{7}$$

The second term in this expression is the area of the conical convergence section and this term becomes significant at higher massflows for larger CR values. As one may expect, both results are linearly dependent on the lengths  $L, L^*$  respectively, and the RDRE chamber is very sensitive to the value of  $\Delta/R_c$ . Here, it is tempting to set a large value in order to reduce surface area, but large annular gaps tend to lower RDRE performance by providing poorer containment of the detonable mixtures provided by the injection system.

Figure 7 compares overall length and diameter of the two thrust chambers for the inputs in Table 2. The length of the RDE thrust chamber is significantly reduced from the conventional combustor with the reduction becoming more prominent at lower thrust/massflow levels. This is a major benefit for space engine systems that must be housed in an inter-stage structure during launch as the length of said structure is reduced as well. Current/prior vehicles have made use of deployable nozzle skirts in an effort to minimize system length thereby demonstrating the importance of this parameter to space missions. In addition, for lander applications, the length of landing gear is directly proportional to propulsion system length in most vehicle concepts. Length reductions here have a multiplicative benefit. The diameter of the RDE chamber is also somewhat smaller than the CP engine; this ratio is invariant with massflow as both throat and chamber diameters scale linearly with massflow.

A sensitivity study was conducted about the design point outlined in Table 2 for a chamber massflow of 10 kg/s. Parameters in Table 2 were varied as noted to assess impact

on chamber surface area, length and radius ratios for RDRE vs. CP chambers. Results from these parametric studies are summarized in Table 3. The radius ratio is independent of chamber pressure because, if massflow and  $c^*$  are fixed, then the quantity  $P_c A_t$  is also fixed. Length varies a small amount with the changes in chamber dimensions stemming from operating pressure change. The surface area ratio is weakly affected with a greater reduction in surface area occurring at lower  $P_c$  values where large CP chambers are required. Similar arguments hold for  $c^*$  variation because mass flow rate and  $P_c$  are fixed.

Changes in RDRE chamber dimensions ( $L$  and  $\Delta/R_c$ ) have a strong effect on chamber surface area to be cooled, and it is desired to have the shortest possible chamber length and largest possible gap to minimize  $A_c$ . Given the small dimensions of the RDRE chamber, overall dimensions change very little. Total length is dominated by nozzle length and the chamber radius is independent of chamber length  $L$ . The radius does decrease with increasing gap size as the throat area is represented by the product of these two quantities. Here, one is motivated to consider throated RDRE combustors as employed on CP engines. Throated combustors have successfully produced rotating detonations in airbreathing and some RDRE experiments, but our prior work [21] led to a negative outcome as the inclusion of the throat completely removed any detonative behavior. It is believed that acoustic waves reflected off the throat may interact with injector pulsations, but the precise mechanism for the behavior has yet to be determined. Additional efforts in this realm are warranted given the potential to reduce surface area and cooling loads for the RDRE. Adding a throat to the RDRE chamber will also ease ignition and allow some pressure buildup from gas injection/evolution. This advantage may be particularly important for a space engine application.

Changing the contraction area ratio of the CP chamber affects all quantities noted in Table 3. Larger  $CR$  values increase surface area of the CP chamber and hence reduce the wall area ratio. While total length is still dominated by the nozzle, larger contraction ratios actually lead to greater length reductions for the RDRE. While the barrel section of the CP chamber shortens with increased contraction ratio, the conical convergence section increases such that the total chamber length from the injector face to the throat reaches a maximum at the  $CR = 4.78$  condition under the assumptions noted. These factors lead to the counterintuitive behavior. Radius ratios obviously are reduced as  $CR$  is increased. Finally, changing the expansion ratio of the terminus of the cooling jacket only affects system length with obvious reductions in length with  $\epsilon_j$ .

## 5. Comparing RDRE and CP Engine Thermal Loads

A prime motivation for this study is to assess the global and local thermal balance in the RDRE as compared to a CP combustor of similar operating pressure and thrust level. The passing of the detonation front over chamber walls thins or removes boundary layers thereby exposing walls to much higher levels of heat transfer than a conventional combustor. In addition, fuel film cooling, a strategy employed in most CP combustors, has not been applied to RDREs to date as there is a fear of parasitic deflagration of the fuel between successive wave arrivals that would have deleterious effects on performance. Heat loads imposed on chamber walls are closely tied to injector design and this raises substantial complications when trying to assess the overall ability to cool the RDRE combustor. The airbreathing RDE community is significantly ahead of the rocket community with numerous publications [26–32] generally showing peak heat transfer at the end of the detonation region, but there are precious few results in the rockets realm with much higher temperature products and much stronger detonation fronts.

The limited results for RDRE applications [9,33,34] tend to leave more questions than answers as they are restricted to specific applications and do not reveal the extent of the cooling problem relative to high-pressure RDRE operation at various thrust levels. Subsequent to publication of our group's study [9], it was determined that the fuel injector utilized was leaking some fuel along the chamber wall so measurements there may be reflective of a fuel film-cooled surface with unknown coolant flowrate. From observed

hardware damage, Stechmann [21] estimated a heat flux about 60% greater than throat level as computed for a CP engine of equivalent conditions. This load is substantial and it is unclear if the total coolant enthalpy, or the local ability to extract the given heat flux, is available for a given application. Gurshin [12] did get closure of the cooling problem for an RL-10 engine application (with assumption regarding detonative heat loads), but scaling to other operating conditions and thrust levels still remains a question.

As engine size/flowrate is diminished, the pressure to which the thrust chamber can be cooled is similarly reduced as engine flow decreases more rapidly than surface area. In the early 1960s, NASA contracted with Marquardt Corporation for a major study of cooling of CP space engines [35]. This comprehensive work considered coolant passage design, chamber materials, propellant combustion characteristics and of course chamber wall heat transfer using tools of the time. Results showed that a LOX/LH<sub>2</sub> fuel-cooled combustor could be operated at a chamber pressure of 400 psi (2.7 MPa) at a thrust level of 800 lbf (3.6 kN) but pressure capability dropped to 40 psi (0.27 MPa) at a thrust level of 70 lbf (310 N) due to reduction in the hydrogen coolant flow.

RDREs will be subject to similar considerations with reduction in operating pressure required for lower thrust missions. Critical heat flux and overall bulk heat loads are the two main top-level thermal considerations. Table 4 summarizes these characteristics as well as critical fluid properties for the liquids considered in the study. A large body of data is available for hydrogen cooling given the large number of engine applications, but notional results are presented from the extensive RL-10 study of Binder [36]. Its excellent cooling characteristics are appreciated by the community as it supports high jacket temperature change as well as heat flux. Methane has received more recent interest [37–39] given the large number of companies pursuing the fuel since the turn of the century, despite methane having cooling characteristics that are quite poor in comparison to hydrogen. This factor, combined with optimal mixture ratios in the 3.3–3.7 range, makes it more demanding to apply to an RDRE. Kerosene [40] has also been studied extensively and is more limited in heat flux capability as a storable liquid. While its critical heat flux is not terribly impressive, it is always employed with fuel film cooling in CP engines and thus the fuel film plays a critical role in reducing heat flux values at high operating pressures. Coking becomes a concern here as well but is beyond the scope of the study that is restricted to looking at a bulk thermal balance or a heat flux limit.

The vast thermal demands for RDRE thrust chambers force one to consider oxidizer cooling and for this reason both oxidizers in the study are listed in Table 4. To be fair, the temperatures quoted are notional at best as propellant subcooling, enthalpy/temperature rise in pump system, and detailed jacket design are all ignored. The notion of critical heat flux is most applicable to low pressure engines where propellant pressures are subcritical in the jacket. Propellant outlet temperatures are drawn from historical data as noted but also can vary substantially with cooling system design.

Especially when considering oxidizers as coolants, jacket material selection and passivation are key requirements for successful implementation. Hydrogen peroxide has seen prior use as a coolant dating back to the 1960s [41–44] in the RMI LR-40 and Rocketdyne AR-2 engines as well as the British Black Knight vehicle. Its monopropellant nature limits temperature rise [42] and its very high critical pressure raises concerns of vapor-locking should the fluid reach its boiling point within the jacket. Extensive work on LOX cooling was conducted at NASA GRC in the 1970s and reveal that it can be an excellent coolant. The end of the cold war revealed Russian successes in this regard and that has spawned modern engines that exploit the ox-rich staged combustion cycle using this fluid. In NASA GRC studies, LOX-cooled combustors were successfully fired at chamber pressures as high as 1200 psi (8.27 MPa) and successful operation was even demonstrated with intentional cooling jacket leaks [45].

**Table 4.** Coolant characteristics from available literature and fluid properties.

Coolant	Coolant Inlet Temp, K	Max Coolant Outlet Temp, K [ref]	Coolant Enthalpy Available, kJ/kg	Critical Pressure, MPa	Critical Heat Flux, kW/cm <sup>2</sup>
LH2	40	250 [25]	2757	1.3	>9
LCH4	111	303 [25]	1920	4.6	1.6 [35]
RP-2	300	670 [39]	744	2.4	0.9 [39]
LOX	90	300 [44]	305	5.0	9.0 [46]
90% HP	300	370 <sup>a</sup> [35]	183	22 (100% HP)	1.27 <sup>b</sup> [35]

<sup>a</sup> → This temperature was for 98% HP. <sup>b</sup> → 90%HP CHF is at 1000 psi.

Cooling approaches employed by the combustor designer will vary with operating conditions, the propellant available for coolant, pressure budget, and material selection to name a few. Each of these considerations will drive the cooling system design, and ultimately impact the operable heat flux and hot wall temperature within the RDE. One of the primary drivers of cooling system performance is the velocity at which the coolant is flowed through the cooling passage. Increasing the velocity of the coolant improves its ability to convect heat from the chamber wall but comes with increased pressure drop. This negatively impacts the feed system designer, requiring either higher performing turbopumps or higher tank pressures. Coolant velocity can be managed by alterations in flowrate or adjusting the total flow area or passes of the cooling passages. Alterations in flowrate are limited as the coolant used in regenerative systems is one or both propellants used for combustor operation and is set by the mixture ratio and total propellant required to meet engine performance. Adjusting the total flow area is the largest knob that can be turned by the cooling system designer and is primarily adjusted by how many channel passes are included in the design.

With many variables, a simplified cooling assessment is presented in Figures 8 and 9. below to make a first-order assessment on a coolants ability to manage heat loads in an RDE. This assessment was completed with a quasi-steady one-dimensional regenerative heat transfer analysis. Heat fluxes were predicted by scaling throat level constant pressure combustor conditions, operating at the same inlet conditions as an RDE. A heat flux scaling factor of 1.6 was developed based on previous analytical studies by Stechman [22]. Coolant velocities were held constant for this study in order to directly compare coolant performance. The velocity selected was 60 m/s as this value is an excessive pressure drop upper limit recommended in NASA SP-8087 [47]. When the designer down selects a coolant, a more detailed study on the cooling channel arrangement and coolant velocity should be completed.

As shown in Figure 8, hydrogen/oxygen systems produce large heat fluxes based on the thermal conductivities of the combustion products. In general, the values here are daunting (as perspective the throat level heat flux of the space shuttle main engine is 8 kW/cm<sup>2</sup> [25]) and with the exception of the low pressures on the left end of the plot values exceed critical heat fluxes shown in Table 4. Almost all CP engines employ fuel film cooling that drastically reduces heat fluxes to the wall and thereby enables high operating pressures. For the RDRE, it is not clear that this is a viable alternative as any fuel injected near the wall may undergo parasitic deflagration thereby robbing some of the performance advantage of the detonative cycle. The 1.6 factor folded into the heat fluxes in Figure 8 is highly speculative and is surely dependent on the injector design employed in studies where this was derived. Nevertheless, the results do indicate the large cooling challenge presented by the RDRE application and the results are a prime factor why a low-pressure space engine may be the most viable initial application of the technology.

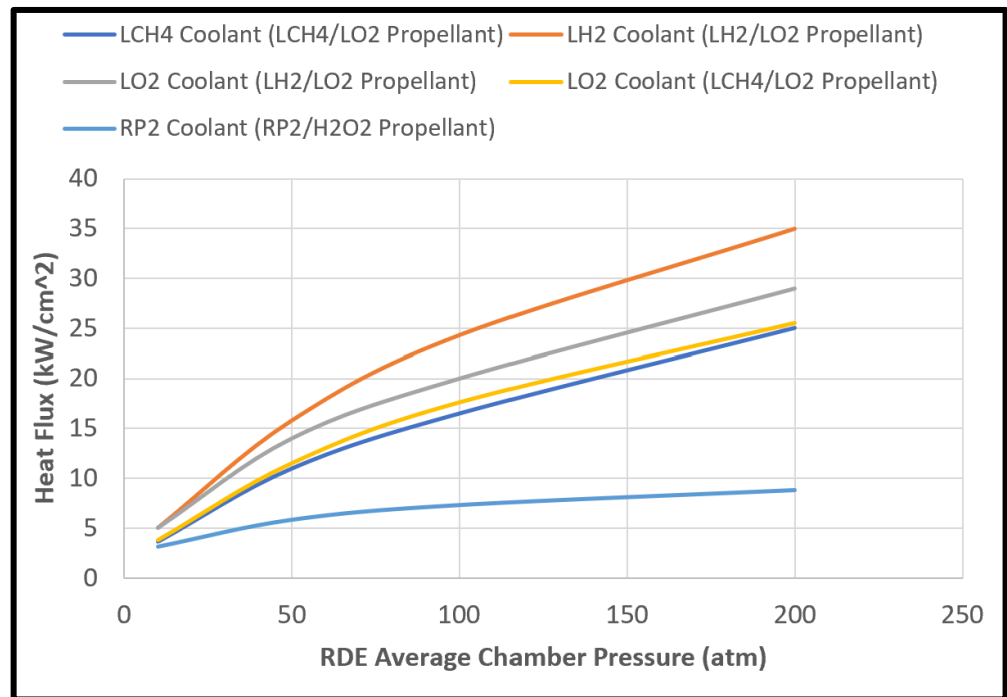


Figure 8. Predicted RDE Heat Flux for Multiple Chamber Pressures and Propellant Combinations.

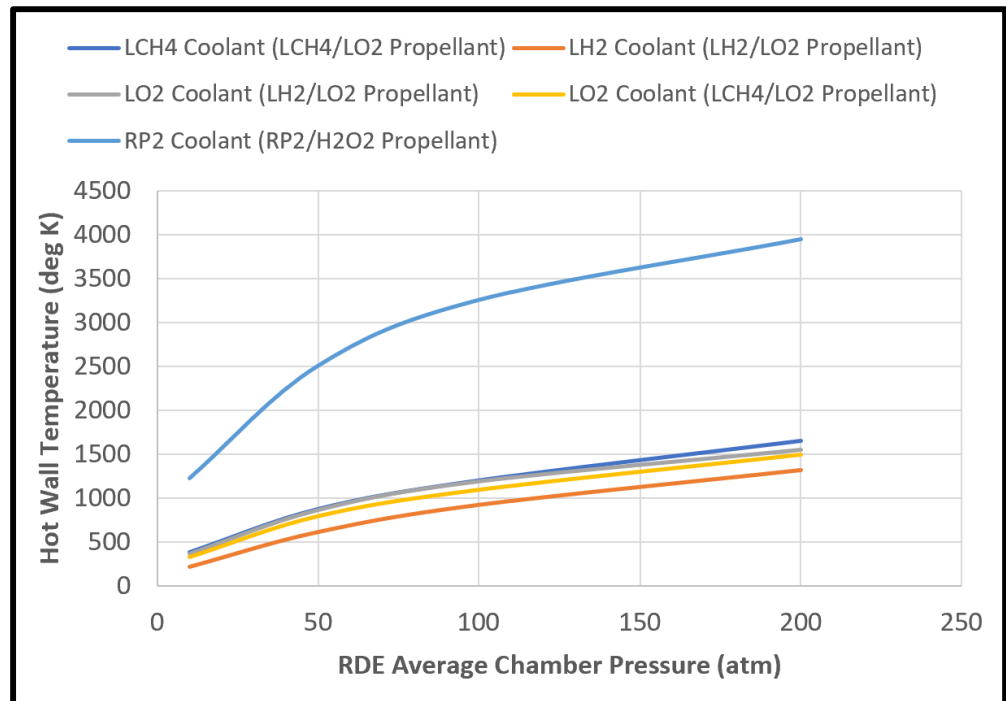


Figure 9. Predicted RDE Hot Wall Temperature for Multiple Chamber Pressures and Propellant Combinations.

The predicted heat flux values for hydrogen/oxygen systems in Figure 8 with hydrogen as the coolant were higher than those with oxygen as the coolant because of the increased cooling capacity of hydrogen lowering the hot wall temperature and increasing the convective heat transfer from the combustion gases. The predicted heat flux from kerosene (RP-2)/hydrogen peroxide system was the lowest and driven primarily by the poor cooling capability of RP-2 raising hot wall temperatures and reducing the convective

heat transfer from the combustion products. In reality, the hot wall temperatures predicted far exceed the material capability and a properly cooled wall would produce considerably higher heat fluxes. Methane/oxygen systems were between the aforementioned propellant combinations with oxygen and methane offering similar cooling capabilities. Heat fluxes for all propellant combinations increase drastically with chamber pressure as expected. Heat fluxes, even at lower chamber pressures on the order of 10 atm, approach or exceed the critical heat fluxes described in Table 4. This is a strong indication of why film cooling is used in high-pressure constant-pressure combustors and should certainly be studied in RDREs. Alternate approaches such as film cooling will likely be critical to long-term operation of RDRE devices at high chamber pressures.

Figure 9 highlights the cooling capabilities of multiple coolants with higher performing coolants able to keep hot wall temperatures lower. This study was completed assuming the chamber material was GRCo-42 where hot wall temperatures are recommended to remain below 1000 K. As shown in the figure, this temperature is exceeded for all coolants at medium to high chamber pressures. This even further highlights the need for additional cooling methods such as film or transpiration cooling in high-pressure RDEs. RP-2 resulted in the worst performing coolant, with wall temperatures exceeding acceptable levels even at low chamber pressures (~10 atm).

As shown Figures 8 and 9, the RDE cooling system designer will be limited in chamber pressure without the use of alternative cooling methods such as film cooling or transpiration cooling. Chamber pressures larger than ~10 atm produce heat fluxes exceeded the critical heat fluxes of available coolants. Given the vacuum of space for expansion of combustion gases, space engines do not sustain large performance degradation at these operating pressures—as an example the famed lunar module descent engine used in the Apollo program had a chamber pressure of only 100 psi (6.8 atm). System-level performance issues become a consideration that is beyond the scope of this paper. For example, regenerative cooling systems necessitate operation at supercritical conditions in many cases thereby dictating certain pressure levels regardless of combustor operating pressure. Even if critical heat flux can be mitigated, hot wall temperatures will limit the RDE combustor designer to ~100 atm with a well performing coolant. Combustor operation exceeding ~100 atm will likely need to employ film or transpiration cooling methods but their impact on combustor performance is yet to be determined.

## 6. Conclusions

Potential performance advantages for a rotating detonation rocket engine (RDRE) conceived for space propulsion applications have been studied. Existing performance models show theoretical specific impulse gains of 3–14% using a model that takes into account quasi-steady nozzle performance for the range of pressures presented in a notional RDRE pressure pulse. Advantages tend to be greatest for hydrogen fuel, but the optimum is driven to very fuel rich conditions for the detonative cycle. Thrust-chamber sizing comparisons reveal that the RDRE enjoys a substantial length reduction when compared to a constant pressure (CP) combustion device for a given thrust level. This advantage is important for space missions, including surface lander applications that would profit by reduction in landing gear length coincident with engine length reductions. While roughly an order of magnitude smaller in volume than a CP combustor, the annular RDRE combustor is shown to have lower surface area over a range of thrust levels pertinent to space propulsion. The RDRE surface area advantage is reduced as thruster size/thrust level is reduced.

Despite potential reductions in cooling surface area, the very high heat loads imposed by the passing detonation front pose substantial challenges in terms of exceeding critical heat fluxes or total available enthalpy for a given application. Here, the lack of data on actual RDRE heat loads impairs our ability to provide firm quantitative information in many cases, but using the limited results obtained thus far reveal that RDRE space engines will be limited to low operating pressures to achieve thermal balance. Nevertheless, prior

history of space engine developments in this realm, combined with the attractive specific impulse that may be attained, does give justification for further study of the RDRE space engine. Transpiration or film cooling approaches that have been applied/studied in CP engines should be explored in the RDRE as they can reduce overall heat loads imposed in the cooling jacket. Here, the introduction of fuel prior to passage of the detonation front raises the potential for parasitic deflagration that could reduce or eliminate any performance advantage that may exist over the CP engine.

**Author Contributions:** Conceptualization, all authors; formal analysis, J.S., K.D., A.H.; investigation, N.B., A.M.; writing—original draft preparation, S.D.H., J.S., K.D.; writing—review and editing, N.B., A.M. funding acquisition, S.D.H. All authors have read and agreed to the published version of the manuscript.

**Funding:** Authors acknowledge support from U.S. Air Force Office of Scientific Research, Air Force Research Lab, NASA, and Purdue University.

**Institutional Review Board Statement:** Not applicable.

**Informed Consent Statement:** Not applicable.

**Data Availability Statement:** Not applicable.

**Conflicts of Interest:** The authors declare no conflict of interest.

## References

- Zeldovich, Y.B. To the Question of Energy Use of Detonation Combustion. Translation of article originally published in Russian in *Zhurnal Tekhnicheskoi Fiziki* (Journal of Technical Physics) Vol. 10, No. 17, 1940, pp. 1453–1461. *J. Propuls. Power* **2006**, *22*, 588–592. [[CrossRef](#)]
- Voitesekhovskii, B.V. Stationary Spin Detonation. *Sov. J. Appl. Mech. Tech. Phys.* **1960**, *3*, 157–164. (In Russian)
- Nicholls, J.A.; Cullen, R.E.; Ragland, K.W. Feasibility studies of a rotating detonation wave rocket motor. *J. Spacecr. Rocket.* **1966**, *3*, 893–898. [[CrossRef](#)]
- Bykovskii, F.A.; Zhdan, S.A.; Vedernikov, E.F. Continuous spin detonations. *J. Propuls. Power* **2006**, *22*, 1204–1216. [[CrossRef](#)]
- Lu, F.K.; Braun, E.M. Rotating detonation wave propulsion: Experimental challenges, modeling, and engine concepts. *J. Propuls. Power* **2014**, *30*, 1125–1142. [[CrossRef](#)]
- Xue, S.; Liu, H.; Zhou, L.; Yang, W.; Hu, H.; Yan, Y. Experimental research on rotating detonation with liquid hypergolic propellants. *Chin. J. Aeronaut.* **2018**, *31*, 2199–2205. [[CrossRef](#)]
- Nair, A.P.; Keller, A.R.; Lima, A.; Spearrin, R.M. Deflagration-to-detonation transition in an annular combustor with hypergolic propellants. In Proceedings of the AIAA SCITECH 2022 Forum, San Diego, CA, USA, 3–7 January 2022.
- Kubicki, S.W.; Anderson, W.; Heister, S.D. Further Experimental Study of a Hypergolic-Ignited Liquid-Liquid Rotating Detonation Rocket Engine. In Proceedings of the AIAA Scitech 2020 Forum, Orlando, FL, USA, 6–10 January 2020.
- Lim, D.; Heister, S.D.; Humble, J.; Harroun, A.J. Experimental Investigation of Wall Heat Flux in a Rotating Detonation Rocket Engine. *J. Spacecr. Rocket.* **2021**, *58*, 1444–1452. [[CrossRef](#)]
- Buyakofu, V.; Matsuoka, K.; Matsuyama, K.; Goto, K.; Kawasaki, A.; Watanabe, H.; Ishihara, K.; Noda, T.; Kasahara, J.; Matsuo, A.; et al. Flight Demonstration of Detonation Engine System Using Sounding Rocket S-520-31: Performance of Rotating Detonation Engine. In Proceedings of the AIAA SCITECH 2022 Forum, San Diego, CA, USA, 3–7 January 2022; p. 0232.
- Kawalec, M.; Perkowski, W.; Łukasik, B.; Bilar, A.; Wolański, P. Applications of the Continuously Rotating Detonation to Combustion Engines at the Łukasiewicz—Institute of Aviation. *Combust. Engines* **2022**, *191*, 51–57. [[CrossRef](#)]
- Gurshin, T. Heating and Regenerative Cooling Model for a Rotating Detonation Engine Designed for Upper Stage Performance. Master's Thesis, Purdue University, West Lafayette, IN, USA, August 2019.
- Andrews, G.; Black, A.; Graham, J.; Rique, O. Preliminary design of a rotating detonation engine for launch vehicle applications. In Proceedings of the 2018 AIAA Aerospace Sciences Meeting, Kissimmee, FL, USA, 8–12 January 2018.
- McBride, B.J. *Computer Program for Calculation of Complex Chemical Equilibrium Compositions and Applications*; NASA Lewis Research Center: Cleveland, OH, USA, 1996; Volume 2.
- Bastea, S.; Fried, L.E.; Glaesemann, K.R.; Howard, W.M.; Kuo, I.W.; Souers, P.C.; Vitello, P.A. *Cheetah 8.0 User's Manual*; Document: LLNL-SM-677152; Energetic Materials Center; Lawrence Livermore National Laboratory: Livermore, CA, USA, 13 October 2015.
- Lee, J.H.S. *The Detonation Phenomenon*; Cambridge University Press: Cambridge, UK, 2008.
- Dille, K.; Harroun, A.; Kubicki, S.W.; Heister, S.D.; Austin, B.L. Development of Condensed Phase Detonation Performance Models for Rotating Detonation Rocket Engines. In Proceedings of the AIAA Scitech 2021 Forum, Virtual Event, 11–15 and 19–21 January 2021.
- Harroun, A.; Heister, S.D. Liquid Fuel Survey for Rotating Detonation Rocket Engines. In Proceedings of the AIAA SCITECH 2022 Forum, San Diego, CA, USA, 3–7 January 2022.

19. Paxson, D.E.; Perkins, H.D. A Simple Model for Rotating Detonation Rocket Engine Sizing and Performance Estimates. In Proceedings of the AIAA Scitech 2021 Forum, Virtual Event, 11–15 and 19–21 January 2021.
20. Harroun, A.J.; Heister, S.D.; Ruf, J.H. Computational and Experimental Study of Nozzle Performance for Rotating Detonation Rocket Engines. *J. Propuls. Power* **2021**, *37*, 660–673. [[CrossRef](#)]
21. Stechmann, D.P. Experimental Study of High-Pressure Rotating Detonation Combustion in Rocket Environments. Ph.D. Thesis, Purdue University, West Lafayette, IN, USA, 2017.
22. Stechmann, D.P.; Heister, S.D.; Harroun, A.J. Rotating Detonation Engine Performance Model for Rocket Applications. *J. Spacecr. Rocket.* **2019**, *56*, 887–898. [[CrossRef](#)]
23. Dille, K. Dynamic Response of Gas/Liquid Injectors at High Pressure Conditions. Master's Thesis, Purdue University, West Lafayette, IN, USA, December 2020.
24. Kindracki, J. Experimental research on rotating detonation in liquid fuel–gaseous air mixtures. *Aerosp. Sci. Technol.* **2015**, *43*, 445–453. [[CrossRef](#)]
25. Heister, S.D.; Anderson, W.E.; Pourpoint, T.L.; Cassady, R.J. *Rocket Propulsion*; Cambridge University Press: Cambridge, UK, 2019; Volume 47.
26. Theuerkauf, S.W.; Schauer, F.; Anthony, R.J.; Paxson, D.E.; Stevens, C.A.; Hoke, J. Comparison of simulated and measured instantaneous heat flux in a rotating detonation engine. In Proceedings of the 54th AIAA Aerospace Sciences Meeting, San Diego, CA, USA, 4–8 January 2016; p. 1200.
27. Meyer, S.J.; Polanka, M.D.; Schauer, F.; Anthony, R.J.; Stevens, C.A.; Hoke, J.; Rein, K.D. Experimental characterization of heat transfer coefficients in a rotating detonation engine. In Proceedings of the 55th AIAA Aerospace Sciences Meeting, Grapevine, TX, USA, 9–13 January 2017; p. 1285.
28. Stevens, C.A.; Fotia, M.; Hoke, J.; Schauer, F. Quasi Steady Heat Transfer Measurements in an RDE. In Proceedings of the 2018 AIAA Aerospace Sciences Meeting, Kissimmee, FL, USA, 8–12 January 2018; p. 1884.
29. Stevens, C.A.; Fotia, M.; Hoke, J.; Schauer, F. An experimental comparison of the inner and outer wall heat flux in an rde. In Proceedings of the AIAA SciTech 2019 Forum, San Diego, CA, USA, 7–11 January 2019; p. 1252.
30. Roy, A.; Strakey, P.; Sidwell, T.; Ferguson, D.H. Unsteady heat transfer analysis to predict combustor wall temperature in rotating detonation engine. In Proceedings of the 51st AIAA/SAE/ASEE Joint Propulsion Conference, Orlando, FL, USA, 27–29 July 2015; p. 4191.
31. Randall, S.; Anand, V.; St George, A.C.; Gutmark, E.J. Numerical study of heat transfer in a rotating detonation combustor. In Proceedings of the 53rd AIAA Aerospace Sciences Meeting, Kissimmee, FL, USA, 5–9 January 2015; p. 0880.
32. Zhou, S.; Ma, H.; Liu, C.; Zhou, C.; Liu, D. Experimental investigation on the temperature and heat-transfer characteristics of rotating-detonation-combustor outer wall. *Int. J. Hydrogen Energy* **2018**, *43*, 21079–21089. [[CrossRef](#)]
33. Bykovskii, F.A.; Vedernikov, E.F. Heat Fluxes to Combustor Walls during Continuous Spin Detonation of Fuel–Air Mixtures. *Combust. Explos. Shock Waves* **2009**, *45*, 70–77. [[CrossRef](#)]
34. Goto, K.; Nishimura, J.; Kawasaki, A.; Matsuo, K.; Kasahara, J.; Matsuo, A.; Funaki, I.; Nakata, D.; Uchiumi, M.; Higashino, K. Propulsive performance and heating environment of rotating detonation engine with various nozzles. *J. Propuls. Power* **2019**, *35*, 213–223. [[CrossRef](#)]
35. Batha, D.R.; Campbell, J.G.; Carey, M.D.; Coulbert, C.D. Thrust Chamber Cooling Techniques for Spacecraft Engines. *Marquardt Corp. Rep.* **1963**, *1*, 5981.
36. Binder, M.; Tomsik, T.; Veres, J.P. *RL10A-3-3A Rocket Engine Modeling Project*; No. NAS 1.15: 107318; NASA: Washington, DC, USA, 1997.
37. Van Noord, J. *A Heat Transfer Investigation of Liquid and Two-Phase Methane*; NASA/TM-2010-216918; NASA Glenn Research Center: Cleveland, OH, USA, 2010.
38. Trejo, A.; Garcia, C.; Choudhuri, A. Experimental investigation of transient forced convection of liquid methane in a channel at high heat flux conditions. *Exp. Heat Transf.* **2016**, *29*, 97–112. [[CrossRef](#)]
39. Gu, H.; Li, H.; Wang, H.; Luo, Y. Experimental investigation on convective heat transfer from a horizontal miniature tube to methane at supercritical pressures. *Appl. Therm. Eng.* **2013**, *58*, 490–498. [[CrossRef](#)]
40. Stiegemeier, B.; Meyer, M.; Taghavi, R. A thermal stability and heat transfer investigation of five hydrocarbon fuels. In Proceedings of the 38th AIAA/ASME/SAE/ASEE Joint Propulsion Conference & Exhibit, Indianapolis, IN, USA, 7–10 July 2002; p. 3873.
41. Ventura, M.; Mullens, P. The use of hydrogen peroxide for propulsion and power. In Proceedings of the 35th Joint Propulsion Conference and Exhibit, Los Angeles, CA, USA, 20–24 June 1999; p. 2880.
42. McCormick, J. *Hydrogen Peroxide Rocket Manual*; Hydrogen Peroxide Division, 12000 Bay Area Blvd, Pasadena, TX (Reprint of 1965 Version of Manual from Becco Corporation); FMC Corporation: Buffalo, NY, USA, 2004.
43. Becklake, J. The British Black Knight Rocket. *J. Br. Interplanet. Soc.* **1990**, *43*, 283–290.
44. Wu, P.K.; Fuller, R.; Morlan, P.; Ruttie, D.; Nejad, A.; Anderson, W. Development of a pressure-fed rocket engine using hydrogen peroxide and JP-8. In Proceedings of the 35th Joint Propulsion Conference and Exhibit, Los Angeles, CA, USA, 20–24 June 1999; p. 2877.
45. Price, H.G. Cooling of high-pressure rocket thrust chambers with liquid oxygen. *J. Spacecr. Rockets* **1981**, *18*, 338–343. [[CrossRef](#)]
46. Spencer, R.G.; Rousar, D.C.; Price, H.G. LOX-Cooled Thrust Chamber Technology Developments. *J. Spacecr. Rockets* **1980**, *17*, 35–41. [[CrossRef](#)]
47. NASA. *Liquid Rocket Engine Fluid-Cooled Combustion Chambers*; NASA SP-8087; NASA: Washington, DC, USA, 1972.